Supplementary Material

MOF-derived spindle-shaped Z-scheme $ZnO/ZnFe_2O_4$ heterojunction: a magnetic recovery photocatalyst for efficient tetracycline hydrochloride degradation

Shilong Suo [1], Wenmei Ma [1] Siyi Zhang [1], Ziwu Han [1], Yumin Wang [1], Yuanyuan Li [1], Yi Xiong [2], Yong Liu [1], Chunqing He [1], Pengfei Fang [1,*]

1 School of Physics and Technology, Key Laboratory of Nuclear Solid State Physics Hubei Province, Wuhan University, Wuhan 430072, China; fangpf@whu.edu.cn (P. F.)
2 School of Mathematical & Physical Sciences, Department of Microelectronics, Wuhan Textile University, Wuhan, 430073, Hubei, China; xiong@wtu.edu.cn (Y.X.)
* Corresponding: fangpf@whu.edu.cn (Pengfei Fang)

Text S1 characterizations

X-ray diffraction (XRD) measurements were collected on a Rigaku-Smart Lab equipped with D/tex Ultra250 detector with 3kW X-ray generator, and recorded from 10° to 80° with the scanning rate of 6°/min. X-ray photoelectron spectra (XPS) were recorded on a Thermo 163 Fisher ESCALAB 250Xi system. Scanning electron microscopy (SEM) images and EDX data were recorded on a FEI Quanta 250 FEG instrument. High-resolution transmission electron microscopy (HRTEM) images were recorded on JEM-2100 electron microscope (JEOL JEM-2100Plus, Japan). The reflectance spectra of all samples over the 190-900 nm range were gained by a UV-visible spectrometer equipped with a Labsphere diffuse reflectance accessory (UV-2550, Shimadzu, Japan), using BaSO4 as the reference standard. The hysteresis loop was measured by a comprehensive physical property test system (PPMS-9,Quantum Design China). The steady-state photoluminescence (PL) spectra of the sample at room temperature were studied with a fluorescence spectrophotometer (Hitachi 4600).

Text S2 Photocatalytic activity measurements

Typically, 20 mg of the photocatalyst was dispersed into 50 mL of TC aqueous solution (100 mg/L). The mixture was stirred in the dark for 30 min to reach the adsorption–desorption equilibrium prior to light irradiation, the suspension was irradiated under a Xenon lamp (XL, 300 W) coupled with an optical cut-off filter ($\lambda \geq 400$ nm). 1 mL of the solution was collected at an interval of 30 min. Subsequently, The obtained solution was centrifuged at 12000 rad/min for 1 min, 0.8 ml supernatant was taken and diluted with 0.8 ml deionized water and analyzed by the UV–Vis spectrophotometer at 357 nm.

Text S3 Photo-electrochemical measurements

The photoelectrochemical measurements (PEC) performances of as-prepared photocatalyst were examined in a 3-arm PEC cell on electrochemical workstation (CSStudio5, CorrTest, WuHan) with the photocatalyst as working electrode, a Pt slice as the counter electrode, and a saturated calomel electrode (SCE) as the reference.

$$E_{NHE} = E_{SCE} + 0.05916 \times pH + 0.241 \ (pH = 7) \quad (S1)$$

The working electrode was prepared via spin-coated slurry onto 1.0 cm × 2.0 cm Indium tin oxide (ITO) glass followed by drying naturally. The slurry was designed by ultrasonically dissolving 10 mg of the photocatalyst and 80 μL (5%) Nafion solution into 1 mL isopropanol. A 300 W Xe lamp with a 400 nm cut-off filter was used as a light source. When 0.5 M Na_2SO_4 aqueous solution as electrolyte, the transient photocurrent-time (I-t) tests with an electrical bias potential of 0.1 eV vs. SCE, Mott-Schottky (M-S) measurements at the frequency of 1000, 2000 and 3000 Hz with the scanning rate of 0.02 V/s and voltage ranging from -1 ~ 1 V and the linear sweep voltammetry (LSV) were performed with a scanning rate of 10 mV/s and the hydrogen evolution voltage ranging from -1 ~ 0 V. In the 0.1 M Na_2S and 0.1 M Na_2SO_3 mixed solution, the electrochemical impedance spectroscopy (EIS) measurements were performed under an ac amplitude of 10 mV and the frequency range from 10^{-1} Hz to 10^5 Hz.

Text S4 Photothermal conversion performance

The photothermal conversion performance can be described by the photothermal conversion efficiency (ŋ), which can be calculated using the following equation [S1]:

$$ŋ = \frac{(Teq-Tam)mcB}{AS} \quad (S2)$$

where c, m, A, S, Tam, and Teq denote the specific heat capacity, mass of the base liquid, total area of heat dissipation, light intensity, ambient temperature, and equilibrium temperature, respectively. For **Eq. S2** in the manuscript, c, m, A, and S were 4.18×10^3 $J\bullet g^{-1}\bullet°C^{-1}$, 48.6 g, 86.39 cm^2, and 564.33 $W\cdot m^{-2}$, respectively. The light intensity was measured by the five-hole method. Parameter B is calculated from **Eqs. 3-5**, and the results are shown in **Fig. S5**.

$$B \equiv \frac{hA_{dis}}{\sum_i m_i c_i} \quad (S3)$$

$$\frac{T(t)-T_{am}}{T_{eq}-T_{am}} = \exp(-Bt) \quad (S4)$$

Text S5 TA-PL analysis method

The 20mg catalyst was dispersed in 50ml aqueous solution containing 2×10^{-3} M NaOH and 5×10^{-4} M TA. After reacting for a period of time according to the required conditions, take 3 ml supernatant. The hydroxyl content can be determined by measuring the luminescence intensity at 425 nm at the excitation wavelength of 315 nm.

Table S1 Comparison of the catalytic performance.

Catalyst	Concentration （mg/L）	Catalyst dosage (g/L)	Light source	Time (min)	Removal rate (%)	Degradation Rate * (%/min)	Ref
ZFF2	100.0	0.400	300 W Xe lamp (λ≥400 nm)	75.0	86.3	0.288	This work
ZO_v/ZFO_v 500	88.8	0.400	300 W Xe lamp (λ≥420 nm)	120.0	82.0	0.152	[S2]
$Fe_2O_3/g\text{-}C_3N_4$	10.0	0.500	500 W xenon lamp (λ≥420 nm)	120.0	73.8	0.012	[S3]
Bi/ZF/BFT	44.4	0.400	300 W Xe lamp (λ≥420 nm)	60.0	81.5	0.151	[S4]
CdS/NC−T	40.0	0.200	300 W Xe–arc lamp (λ≥420 nm)	60.0	83.0	0.277	[S5]
$Ag_3PO_4/CuBi_2O_4$	20.0	0.500	300 W xenon lamp (λ≥420 nm)	60.0	75.0	0.050	[S6]
$Ag@g\text{-}C_3N_4@BiVO_4$	20.0	0.300	300 W xenon lamp (λ≥420 nm)	60.0	82.8	0.092	[S7]
$ZnO\text{-}ZnFe_2O_4$-60	25.0	0.150	500 W Halogen lamp	240.0	93.68	0.065	[S8]
0.6-ZBO	40.0	0.200	300 W Xe lamp (λ≥400 nm)	90.0	85.6	0.186	[S9]

*Degradation Rate=Concentration×Removal rate/(Catalyst dosage×Time)

Table S2 The main elements contained in tap water

Detection index	Detection result	Detection index	Detection result	Detection index	Detection result
As (mg/L)	0.0014	Cd (mg/L)	<0.0001	Cr^{6+} (mg/L)	<0.004
Ba (mg/L)	0.056	B (mg/L)	0.065	Mo (mg/L)	0.0015
Zn (mg/L)	<0.001	Al (mg/L)	0.088	pH	7.82
Mn (mg/L)	0.0001	Fe (mg/L)	0.011	Cu (mg/L)	0.0008
Chlorate (mg/L)	0.08	Chloride (mg/L)	32.8	Sulfate (mg/L)	52.2
Permanganate (mg/L)	0.92	Ammonia (mg/L)	<0.02	Free chlorine (mg/L)	0.65
Fluoride (mg/L)	0.16	Nitrate (mg/L)	2.15	Na (mg/L)	28.6
Ni (mg/L)	0.0004	Ag (mg/L)	<0.0001		

Table S3 Scavengers used and oxidizing species quenched.

Scavengers	ROSs quenched	Scavenger dosage
Isopropanol (IPA)	$\bullet O^{2-}$	0.1M
Benzoquinone(BQ)	•OH	0.1 mM
Triethanolamine(TEOA)	h^+	0.1M
Silver nitrate ($AgNO_3$)	e^-	0.1M

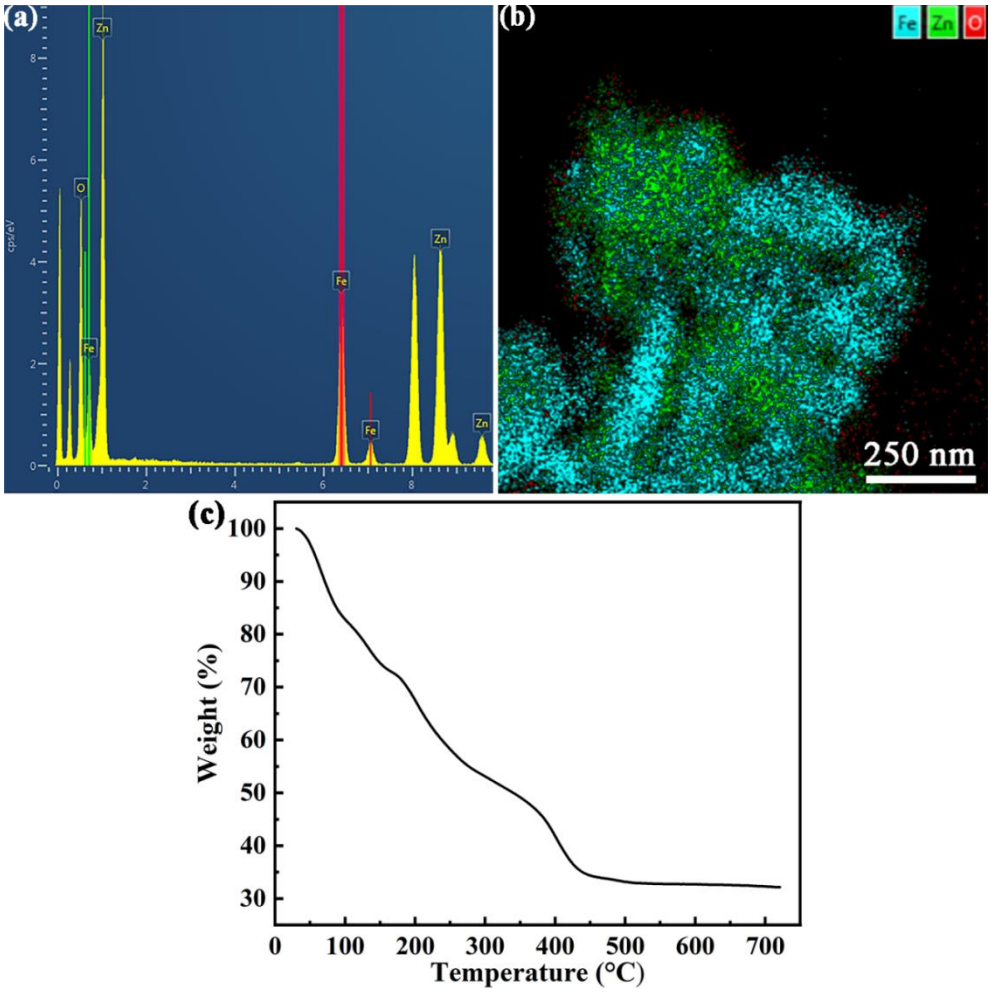

Figure S1. (a) EDS spectra and (b) EDX mapping of ZZF2. (c) Thermogravimetric curve of MIL-88A(Fe)@Zn.

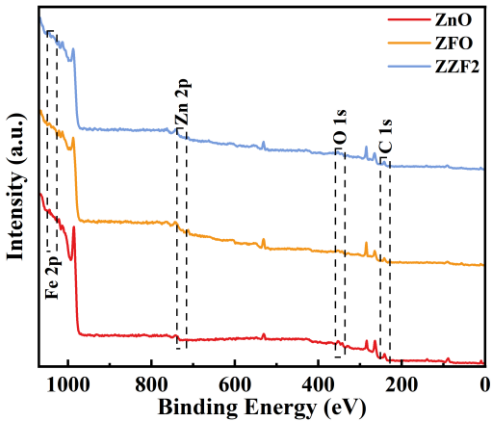

Figure S2. The full XPS survey spectra of $ZnFe_2O_4$, $ZnFe_2O_4$/ZnO heterostructures (sample ZZF2), and ZnO.

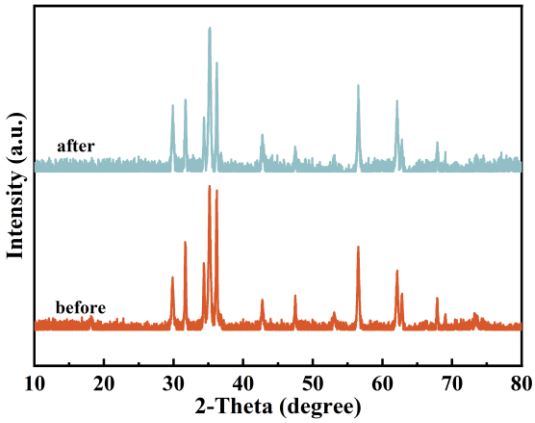

Figure S3. XRD patterns of the fresh ZZF2 and the used one after the 5th-run reaction.

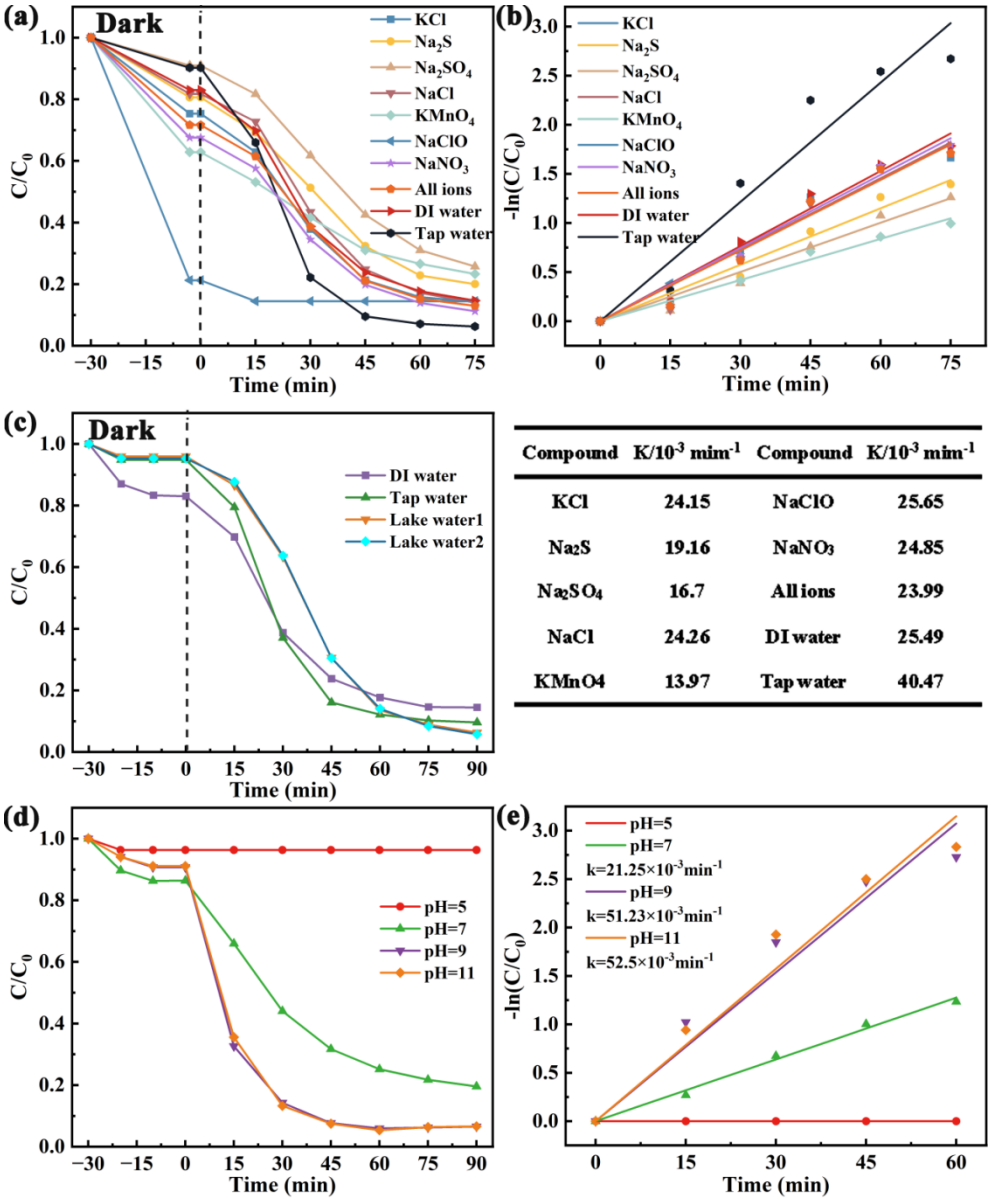

Compound	K/10^{-3} mim^{-1}	Compound	K/10^{-3} mim^{-1}
KCl	24.15	NaClO	25.65
Na_2S	19.16	$NaNO_3$	24.85
Na_2SO_4	16.7	All ions	23.99
NaCl	24.26	DI water	25.49
KMnO4	13.97	Tap water	40.47

Figure S4. (a) Photodegradation performance and (b) degradation rate constants of the ZZF2 at different compound. (c) Degradation effect of the ZZF2 in different water quality. (d) Photodegradation performance and (e) degradation rate constants of the ZZF2 at different pH.

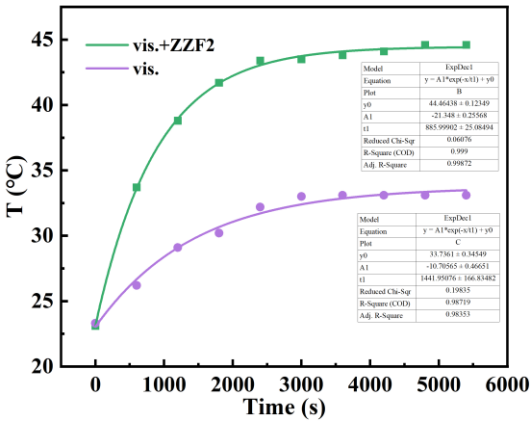

Figure S5. The fitting of parameter B.

$$B=1/t1 \quad \text{(S5)}$$

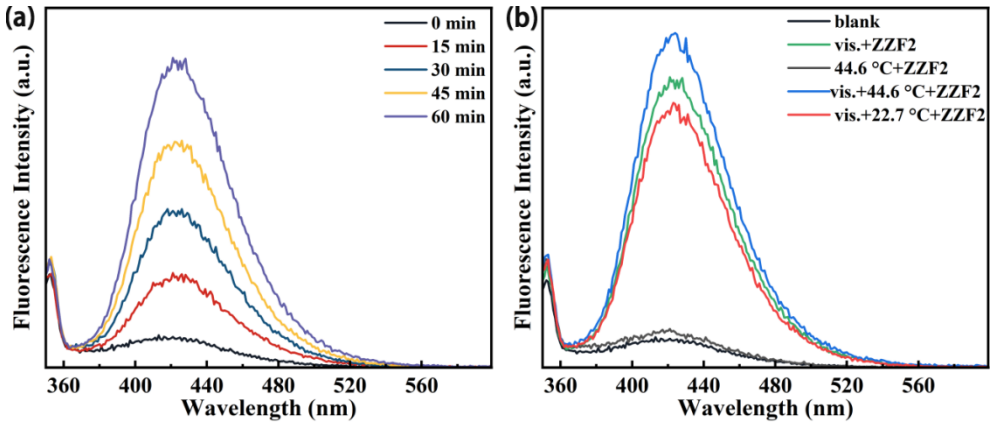

Figure S6. (a) PL spectra depended on the concentration of •OH radical of ZZF2 under visible light irradiation. (b) •OH radical concentration-related PL spectra of ZZF2 under different conditions with visible light irradiation for an hour.

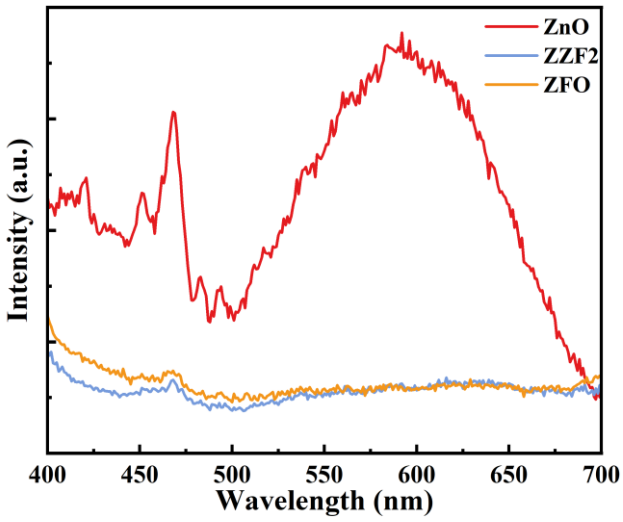

Figure S7. PL spectra of $ZnFe_2O_4$, ZZF2 and ZnO.

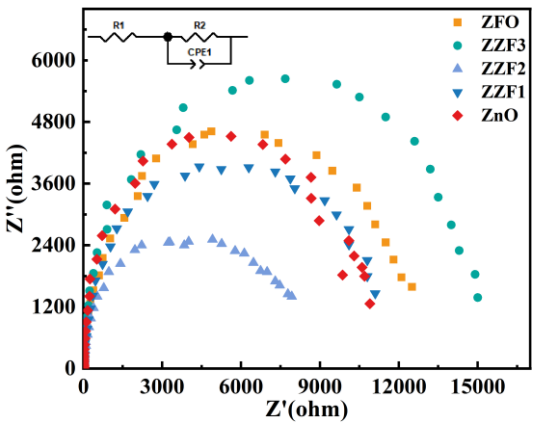

Figure S8. EIS Nyquist plots under darkness of ZnO, ZZF samples and $ZnFe_2O_4$.

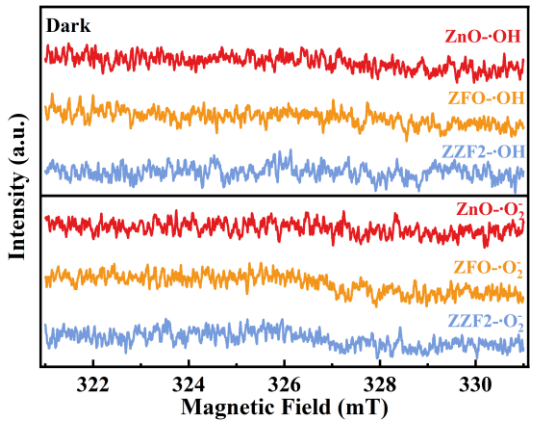

Figure S9. ESR spectra of DMPO -•O2- and DMPO -•OH of ZnO, $ZnFe_2O_4$ and ZZF2 in the dark.

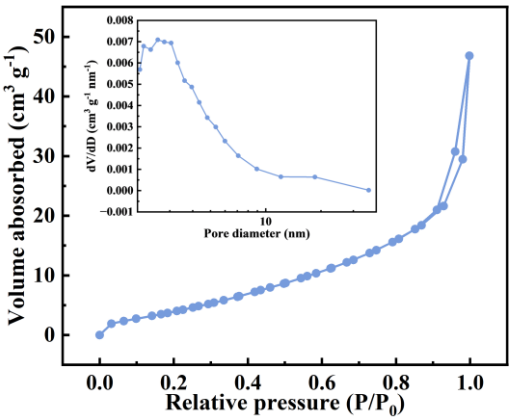

Figure S10. N_2 adsorption–desorption isotherms and pore size distribution curves of ZZF2.

References

1. D.H. Zhu, L. Cai, Z.Y. Sun, A. Zhang, P. Heroux, H. Kim, W. Yu, Y.A. Liu, Efficient degradation of tetracycline by RGO@black titanium dioxide nanofluid via enhanced catalysis and photothermal conversion, *Sci. Total Environ.*, **2021,** *787*. https://doi.org/10.1016/j.scitotenv.2021.147536.
2. K. Zhang, H.Y. Cao, A. Dar, D.Q. Li, L.A. Zhou, C.Y. Wang, Construction of oxygen defective ZnO/$ZnFe_2O_4$ yolk-shell composite with photothermal effect for tetracycline degradation: Performance and mechanism insight, *Chin. Chem. Lett.*, **2023,** *34(1)*. https://doi.org/10.1016/j.cclet.2022.03.031.
3. C. Li, S. Yu, H. Che, X. Zhang, J. Han, Y. Mao, Y. Wang, C. Liu, H. Dong, Fabrication of Z-Scheme Heterojunction by Anchoring Mesoporous γ-Fe_2O_3 Nanospheres on g-C_3N_4 for Degrading Tetracycline Hydrochloride in Water, *ACS Sustain. Chem. Eng.*, **2018,** *6(12),* 16437-16447. https://doi.org/10.1021/acssuschemeng.8b03500.
4. K. Zhang, D. Li, Q. Tian, H. Cao, F. Orudzhev, I.A. Zvereva, J. Xu, C. Wang, Recyclable 0D/2D $ZnFe_2O_4$/$Bi_5FeTi_3O_{15}$ S-scheme heterojunction with bismuth decoration for enhanced visible-light-driven tetracycline photodegradation, *Ceram. Int.*, **2021,** *47(12),* 17109-17119. https://doi.org/https://doi.org/10.1016/j.ceramint.2021.03.020.
5. H.L. Cao, F.Y. Cai, K. Yu, Y.Q. Zhang, J. Lu, R. Cao, Photocatalytic Degradation of Tetracycline Antibiotics over CdS/Nitrogen-Doped-Carbon Composites Derived from in Situ Carbonization of Metal-Organic Frameworks, *ACS Sustain. Chem. Eng.*, **2019,** *7(12),* 10847-+. https://doi.org/10.1021/acssuschemeng.9b01685.
6. W.L. Shi, F. Guo, S.L. Yuan, In situ synthesis of Z-scheme Ag_3PO_4/$CuBi_2O_4$ photocatalysts and enhanced photocatalytic performance for the degradation of tetracycline under visible light irradiation, *Appl. Catal. B-Environ.*, **2017,** *209* 720-728. https://doi.org/10.1016/j.apcatb.2017.03.048.
7. F. Chen, Q. Yang, Y.L. Wang, J.W. Zhao, D.B. Wang, X.M. Li, Z. Guo, H. Wang, Y.C. Deng, C.G. Niu, G.M. Zeng, Novel ternary heterojunction photcocatalyst of Ag nanoparticles and g-C_3N_4 nanosheets co-modified $BiVO_4$ for wider spectrum visible-light photocatalytic degradation of refractory pollutant, *Appl. Catal. B-Environ.*, **2017,** *205* 133-147. https://doi.org/10.1016/j.apcatb.2016.12.017.
8. C. Akshhayya, M.K. Okla, W.H. Al-Qahtani, M.R. Rajeshwari, A. Mohebaldin, Y.A. Alwasel, W. Soufan, M.A. Abdel-Maksoud, H. AbdElgawad, L.L. Raju, A.M. Thomas, S.S. Khan, Novel $ZnFe_2O_4$ decorated on ZnO nanorod: Synergistic photocatalytic degradation of tetracycline, kinetics, degradation pathway and antifungal activity, *J. Environ. Chem. Eng.*, **2022,** *10(3)*. https://doi.org/10.1016/j.jece.2022.107673.
9. J.H. Luo, Y.H. Wu, M.Z. Jiang, A.H. Zhang, X.Y. Chen, Y.L. Zeng, Y.H. Wang, Y.L. Zhao, G.J. Wang, Novel $ZnFe_2O_4$/BC/ZnO photocatalyst for high-efficiency degradation of tetracycline under visible light irradiation, *Chemosphere*, **2023,** *311*. https://doi.org/10.1016/j.chemosphere.2022.137041.